25 Jan 2022

Examining the Effect of a Chitosan Biopolymer on Alkali-Activated Inorganic Material for Aqueous Pb(II) and Zn(II) Sorption

Sukanta K. Mondal

Chenglin Wu
Missouri University of Science and Technology, wuch@mst.edu

Felix C. Nwadire

Ali A. Rownaghi
Missouri University of Science and Technology, rownaghia@mst.edu

et. al. For a complete list of authors, see https://scholarsmine.mst.edu/civarc_enveng_facwork/2367

Recommended Citation

S. K. Mondal et al., "Examining the Effect of a Chitosan Biopolymer on Alkali-Activated Inorganic Material for Aqueous Pb(II) and Zn(II) Sorption," *Langmuir*, vol. 38, no. 3, pp. 903 - 913, American Chemical Society, Jan 2022.
The definitive version is available at https://doi.org/10.1021/acs.langmuir.1c01829

LANGMUIR

pubs.acs.org/Langmuir Article

Examining the Effect of a Chitosan Biopolymer on Alkali-Activated Inorganic Material for Aqueous Pb(II) and Zn(II) Sorption

Sukanta K. Mondal, Chenglin Wu, Felix C. Nwadire, Ali Rownaghi, Aditya Kumar, Yusuf Adewuyi, and Monday U. Okoronkwo*

Cite This: *Langmuir* 2022, 38, 903−913 Read Online

ACCESS | Metrics & More | Article Recommendations

ABSTRACT: Biopolymers and alkali-activated materials have attracted a great deal of attention as adsorbents for the removal of heavy metal contaminants from aqueous solutions. Both materials are sustainable and feature unique properties, but biopolymers are relatively more expensive or difficult to prepare and exhibit low mechanical and surface properties, a narrow pH range, and thermal stability. In this study, hybrid adsorbents were prepared from both types of material, by alkali activation of low-cost fly ash precursors accompanied by incorporation of 0−2%$_{mass}$ chitosan biopolymer. Two types of alkaline activating solutions, NaOH and Na_2SiO_3, were employed to generate two sets of hybrid adsorbents with varying chitosan contents. The effect of the chitosan dosage on the aqueous Pb(II) and Zn(II) sorption efficiency was also investigated. The adsorbents exhibited 98−100% removal efficiencies for both metals, but the sorption of Zn(II) was generally higher than that of Pb(II). The addition of 0.1−2.0%$_{mass}$ chitosan resulted in very little improvement in the overall efficiency of the adsorbents. In contrast, 0.05%$_{mass}$ chitosan led to a decrease in the sorption efficiency; this was linked to the decrease in the adsorbents' ζ potential. The Na_2SiO_3-activated materials featured larger BET surface areas and better overall sorption performance, while the NaOH-activated materials showed the worst Pb(II) sorption performance and hence more noticeable improvement upon addition of chitosan. Mechanistic investigation shows that the sorption process follows second-order kinetics and is a chemisorption-driven process.

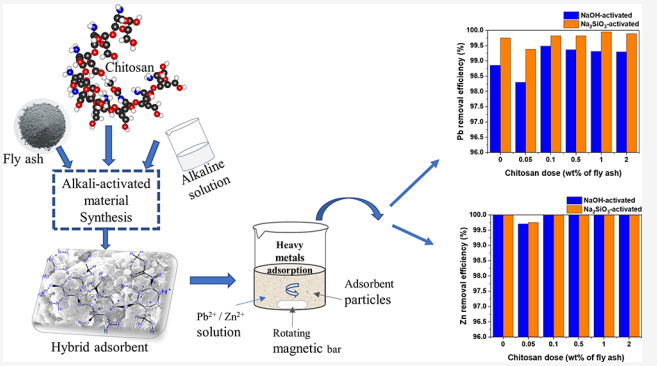

INTRODUCTION

Because of the renewability, biodegradability, nontoxicity, biocompatibility, and functionality, biopolymers have attracted more research attention in the recent decade for applications in many fields, including agriculture,[1] food,[2,3] cosmetics,[4] biomedicine,[5,6] electronics,[7] building,[8,9] and environmental remediation.[10−13] Chitosan, a poly-β-glucosamine biopolymer produced by alkaline deacetylation of chitin derivatives found in the exoskeleton of arthropods,[14,15] has been widely studied for its application in water treatment and contaminant removal.[16−19] Various studies have shown that chitosan exhibits excellent performance in removing cationic heavy metals, e.g., Pb(II),[20,21] oxoanionic heavy metals, e.g., As,[22] and dyes and organic contaminants.[23] However, chitosan as an adsorbent has major drawbacks, including a low porosity and a small surface area, low acid stability and thermal stability, poor mechanical properties, and hydrophilicity.[20,23] As a result, chitosan is often used in composites with inorganics or modified with other materials to address the various deficiencies to produce a robust adsorbent.[17,23,24]

Alkali-activated materials such as geopolymers or poly-sialate inorganic polymers are low-cost materials known to also exhibit excellent performance in removing and immobilizing aqueous heavy metal ions.[25−28] These classes of materials are prepared by reacting aluminosilicate precursors such as fly ash, slag, or calcined clay with alkaline activating solutions.[29−32] The precursors for the alkali-activated materials are comparatively more abundant and less expensive. For example, fly ash, primarily a coal combustion byproduct, costs approximately \$15−25/ton,[33] which is >100 times cheaper than chitin (\$3−6/kg) and commercial chitosan (\$15−20/kg).[34,35] It should be noted that the cost of chitosan can range from \$10 to \$1000/kg depending on quality.[36] Neverthless, as recent techno-economic analyses have shown, the cost of chitosan-based adsorbents can

Received: July 8, 2021
Revised: January 4, 2022
Published: January 13, 2022

https://doi.org/10.1021/acs.langmuir.1c01829
Langmuir 2022, 38, 903−913

Table 1. Compositions of the Precursor Material and the Prepared Adsorbent

(a) Composition Parameters of the Synthesized Adsorbent (molar ratio)							
adsorbent ID	activator type	Ca/Si	Al/Si	Na/Si	Ca/(Si + Al)	(Na + Ca)/ (Si + Al)	chitosan dose ($\%_{mass}$)
C1	10 M NaOH	1.065	0.303	1.315	0.817	1.826	0−2
C2	1 M Na_2SiO_3	0.944	0.269	0.251	0.743	0.942	0−2

(b) Chemical Composition of Precursor Fly Ashes Used ($\%_{mass}$)											
CaO	SiO_2	Al_2O_3	MgO	Fe_2O_3	Na_2O	K_2O	SO_3	P_2O_5	TiO_2	Mn_2O_3	SrO
32.50	32.69	16.83	5.28	6.13	0.95	0.54	1.76	1.47	1.41	0.03	0.38

be reduced via the preparation of its composites with inorganic materials.[37]

Fly ash produced from different industries, mostly from coal-based power plants, presents increasing environmental liability and economic cost for its disposal.[38−40] Conversion and beneficial utilization of fly ash have attracted more attention as a sustainable solution to the problems.[38] Heavy metal exposure is known to pose severe adverse impacts on human health and the environment.[41] Lead pollution has caused serious threats to the biotic system because of its high toxicity and potential mutagenic effects.[42,43] The World Health Organization-set limit of Pb(II) in drinking water is 10 μg/L;[44] however, low-level environmental exposure is still linked to substantial neuro-behavioral problems in children.[45,46] Zinc is another heavy metal generated from multiple sources, largely from chemical industries.[47,48] Although Zn(II) is an essential trace element, when its concentration is greater than the permissible limit of 5 mg/L in water, it may lead to acute toxicity to both aquatic organisms and plants,[49,50] as well as toxicity in humans due to inhibition of copper uptake.[51−53] Therefore, the removal of Pb(II) and Zn(II) from wastewater is often crucial.

Chitosan removes heavy metals via a chemical interaction with the amine and hydroxyl functional groups of its structure,[54] while the alkali-activated inorganic material is known to remove heavy metals through ion exchange and substitution mechanisms.[55,56] Thus, a composite of both materials can potentially benefit from a multifunctional sorption mechanism that may lead to enhanced adsorbent efficiency. However, the limited literature on chitosan-modified alkali-activated materials is mostly focused on the synthesis of concrete or materials for construction applications.[57,58] In this work, composites of alkali-activated fly ash materials and chitosan are prepared and studied to investigate the effect of chitosan on the efficiency of the composite as an adsorbent for Pb(II) and Zn(II) sorption as representative heavy metal ions, wherein the inexpensive alkali-activated fly ash inorganic component constitutes ≥98% of the prepared adsorbent. It is hypothesized that the biopolymer will functionalize the inorganic components, thereby enhancing their sorption efficiency, while the inorganic component will provide enhanced physicomechanical properties, leading to an overall cost-efficient adsorbent. Thus, the primary aim of this study is to test this hypothesis by investigating potential synergistic interactions that may provide mechanistic insights and inform the design of sustainable cost-efficient adsorbents for the removal of heavy metal ions.

EXPERIMENTAL SECTION

Material Development. Two sets of alkali-activated materials with different chitosan dosages were prepared using an ASTM Class C fly ash and reagent grade 10 M NaOH (sodium hydroxide pellets, Fisher Chemical, purity of 98.6%) and 1 M Na_2SiO_3 (sodium meta-silicate pentahydrate, Fisher Chemical, technical grade) alkaline activating solutions (Table 1). A laboratory grade chitosan biopolymer composed of 85% deacetylated chitin, (1,4)-2-amino-2-deoxy-*b*-D-glucan purchased from Carbosynth LLC was used. To prepare the hybrid adsorbents, the fly ash was mixed with each alkaline solution at a solution:solid ratio of 0.7 while chitosan was dosed at 0−2$\%_{mass}$ (i.e., 0%, 0.05%, 0.1%, 0.5%, 1%, and 2%), and the mixture was stirred at 850 rpm for 20 min. The resulting paste was placed in a sealed plastic dish, cured at 90 °C for 24 h, and aged at room temperature for 7 days. After the aging, the adsorbents were pulverized prior to sorption studies. We note that a 10 M NaOH solution is known to sufficiently activate fly ash to produce geopolymers, while a 1 M Na_2SiO_3 solution used singly is uncommon in the literature but has been shown to produce a beneficial highly amorphous adsorbent.[27,59] Reagent grade lead(II) nitrate [$Pb(NO_3)_2$, Alfa Aesar, purity of 99%] and zinc(II) nitrate [$Zn(NO_3)_2{\cdot}6H_2O$, Acros Organics, purity of 98%] were used to prepare the single-ion adsorbate solutions for the sorption studies described below.

Characterization Techniques. The Oxford X-Supreme 8000 X-ray fluorescence (XRF) instrument was used to analyze the oxide composition of the fly ash material, while the PANalytical X'Pert Pro Multi-Purpose Diffractometer was used to obtain the X-ray diffraction (XRD) patterns to reveal the phase assemblage in the prepared adsorbents. For XRD, the samples were scanned with Cu Kα radiation (λ = 1.540 Å) from 5° to 90° 2θ in a continuous manner at an integrated step size of 0.026° 2θ. The surface morphology of the prepared adsorbents was studied using a Hitachi S4700 scanning electron microscope (SEM). The N_2 physisorption isotherm was assessed with a Micrometrics 3Flex gas analyzer at −196 °C to determine the surface properties of the materials. Before measurement, the samples were degassed for 6 h at 50 °C under a vacuum to remove any pre-adsorbed gases and moisture. The specific surface areas (SSA) and pore size distributions (PSDs) were determined by the Brunauer−Emmett−Teller (BET) and nonlocal density functional theory (NLDFT) methods, respectively. ζ potential analysis of the samples was accomplished utilizing the Anton Paar Litesizer 500 dynamic light scattering (DLS) instrument. A Nicolet iS50 Fourier transform infrared (FTIR) instrument was used to record the infrared spectra of prepared adsorbents at wavenumbers from 400 to 4000 cm^{-1} with a resolution of 4 cm^{-1}, using the attenuated total reflection (ATR) method. The elemental analysis was performed with a PerkinElmer AVIO 200 inductively coupled plasma-optical emission spectrometry (ICP-OES) instrument. The spectral line of the elemental Pb 220.353 nm and Zn 213.856 nm was measured, and the mean of triplicate measurements of the aqueous elemental Pb and Zn was obtained. Selected samples with low concentrations were verified with PerkinElmer Analyst 600 graphite furnace atomic absorption spectrophotometer (GFAA) with a detection limit in the range of parts per billion.

Sorption Test. Single-metal ion batch adsorption tests were conducted with a solution with an initial concentration of 100 ppm Pb(II) and another separate solution with an initial concentration of 100 ppm Zn(II), with a 2 g/L adsorbent dosage in each case. The adsorbent dosage of 2 g/L was adopted as it was found to be optimal in several geopolymer-based heavy metal ion removal processes.[60,61] The effect of chitosan dosage and contact time was studied. The adsorbent was dispersed in 50 mL of an adsorbate solution and stirred at 300 rpm for a total contact time of 4 h. The samples were collected at regular time intervals and filtered with a 0.2 μm PTFE filter. Then the Pb(II) and Zn(II) concentration in the filtered aqueous solutions was determined by ICP-OES. Other sorption conditions in this study were kept constant to investigate the effect of chitosan on only the

https://doi.org/10.1021/acs.langmuir.1c01829
Langmuir 2022, 38, 903−913

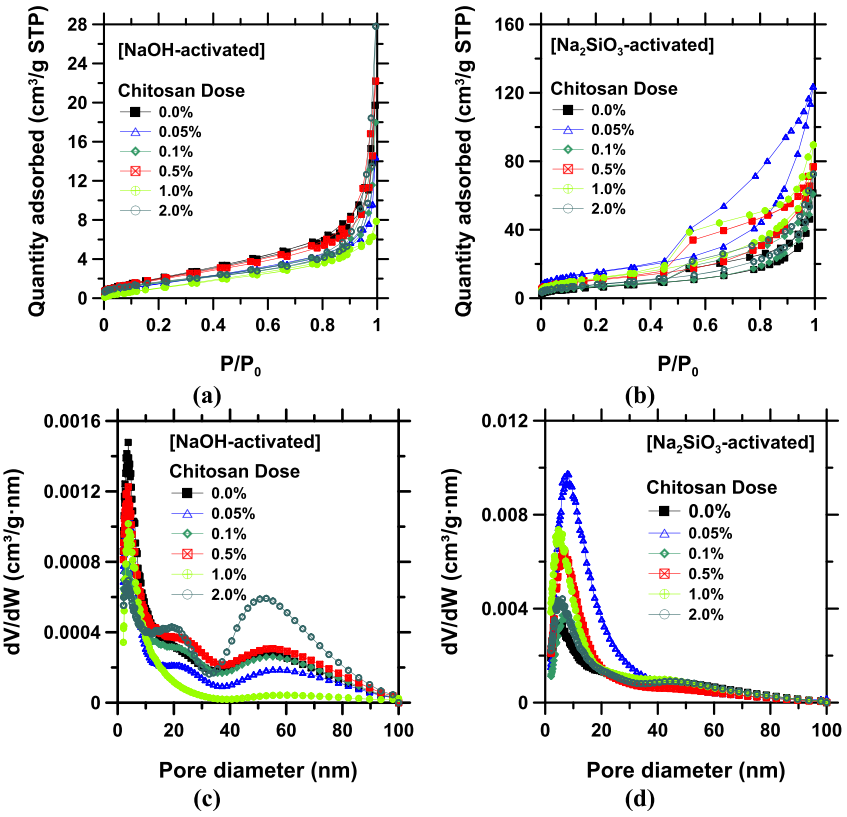

Figure 1. (a and b) N_2 physisorption isotherms. (c and d) Pore size distribution profiles for NaOH-activated and Na_2SiO_3-activated sets of prepared adsorbents.

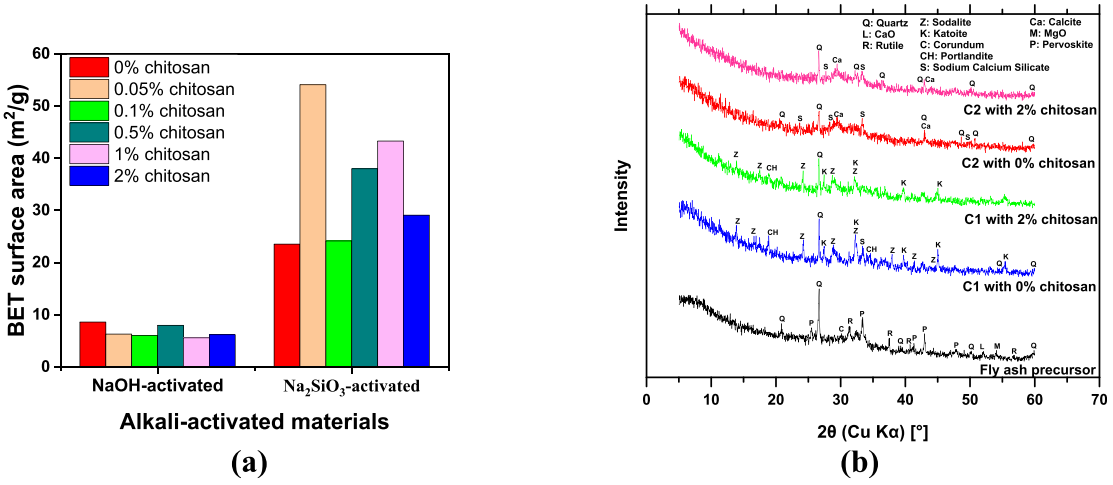

Figure 2. (a) Specific surface area of the NaOH-activated and Na_2SiO_3-activated materials. (b) XRD patterns of raw fly ash and the representatives of the alkali-activated adsorbents containing $0\%_{mass}$ and $2\%_{mass}$ chitosan.

sorption efficiency. The temperature and pH were maintained at preselected values of 40 °C[60] and 7 ± 1,[60,62,63] respectively, as the reported optimum conditions. Deionized water with a resistivity of 18.2 MΩ was used to prepare the synthetic Pb(II) and Zn(II) solutions. The Pb(II) and Zn(II) removal efficiency and time-dependent uptake were calculated as follows:

$$\text{removal efficiency}\,(\%) = \frac{C_0 - C_{eq}}{C_0} \times 100 \quad (1)$$

where C_0 is the initial concentration of Pb(II) or Zn(II) (parts per million) and C_{eq} is the equilibrium concentration (parts per million) of Pb(II) or Zn(II) in the sorption solution.

$$\text{uptake, } q_t = \frac{(C_0 - C_{eq})V}{W} \quad (2)$$

where q_t [milligrams of Pb(II) or milligrams of Zn(II) per gram of geopolymer] is the amount of Pb(II) or Zn(II) uptake by the adsorbent at time t, V is the volume of the sorption solution (liters), and W is the mass of the adsorbent (grams).

RESULTS AND DISCUSSION

Characterization of Prepared Adsorbents. The N_2 adsorption−desorption isotherms of the prepared adsorbents are shown in panels a and b of Figure 1. The isotherms show

https://doi.org/10.1021/acs.langmuir.1c01829
Langmuir 2022, 38, 903−913

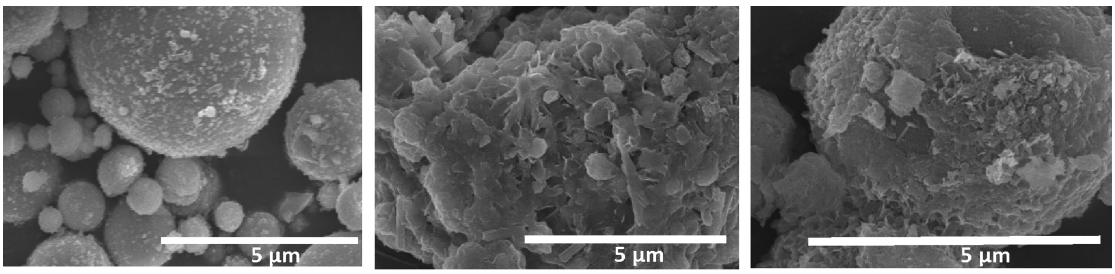

Figure 3. SEM images of (a) the fly ash precursor, (b) 2% chitosan-dosed NaOH-activated material (C1), and (c) 2% chitosan-dosed Na_2SiO_3-activated material (C2).

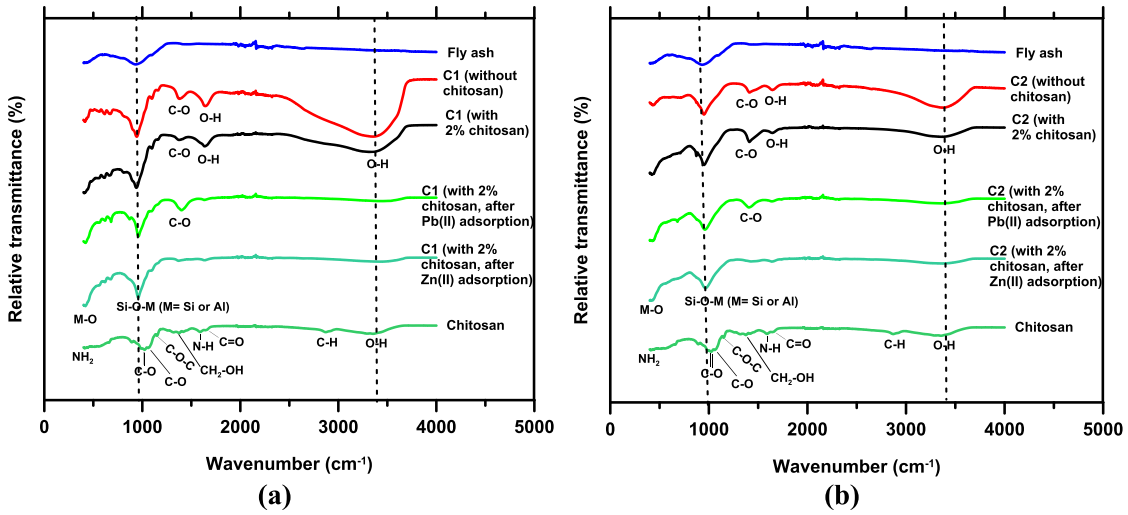

Figure 4. FTIR spectra of fly ash, chitosan, and the adsorbents containing $0\%_{mass}$ and $2\%_{mass}$ chitosan before and after metal ion sorption: (a) NaOH-activated and (b) Na_2SiO_3-activated.

mostly the features of mesoporous materials with a pseudo-type IV isotherm and type H3 hysteresis loop, with a sharp uptake between 0.9 and 1.0 relative pressure (P/P^0).[64] The NaOH-activated adsorbents show a significant amount of pores in the macropore range [>50 nm (Figure 1c)] compared to the Na_2SiO_3-activated materials that feature a pore concentration in the mesopore range [<50 nm (Figure 1d)], hence the more pronounced capillary condensation effect and wider hysteresis loop in the latter. The BET specific surface area is presented in Figure 2a, showing that the Na_2SiO_3-activated adsorbents generally feature surface areas that are larger than those of their corresponding NaOH-activated adsorbents.

The XRD patterns of the fly ash sample and the prepared adsorbents with 0% and $2\%_{mass}$ chitosan are shown in Figure 2b. Most of the crystalline phases in the fly ash precursor reacted to form new crystalline and amorphous phases, but unreacted quartz is still detected in the prepared adsorbents. The NaOH-activated adsorbent shows a higher degree of reaction, presenting new crystalline hydration products (including zeolites and portlandite), whereas the Na_2SiO_3-activated materials show mainly an X-ray amorphous geopolymer-like calcium-(sodium)-alumina-silicate-hydrate [C(N)-A-S-H] gel phase.[65,66] The XRD data suggest a larger surface area for the Na_2SiO_3-activated materials in agreement with the BET data. Previous studies of the unmodified alkali-activated systems[27] have shown that the presence of more amorphous phases leads to higher metal ion sorption. The amorphous geopolymer-like phase features finer pore networks, a larger surface area, and more active sites that enhance sorption in contrast to a coarse crystalline morphology. As shown in Figure 2b, the XRD patterns of the adsorbents containing $0\%_{mass}$ and $2\%_{mass}$ chitosan are quite similar, suggesting that the addition of chitosan had very little impact on the mineral phase assemblage. Thus, the interaction between the chitosan and the alkali-activated fly ash material is possibly a surface phenomenon via hydrogen bonding.[58]

The microstructural images of the fly ash precursor, the synthesized 2%-chitosan-dosed NaOH-activated adsorbent, and 2%-chitosan-dosed Na_2SiO_3-activated adsorbent are shown in Figure 3. As shown in Figure 3, the initial smooth spherical surface of the fly ash particles has transformed after the alkali activation and reaction with chitosan and shows a different degree of reaction in NaOH- and Na_2SiO_3-activated systems. The former shows a high degree of reaction characterized by a more coarse surface morphology compared to the latter (Figure 3b,c), which exhibits more armorphous features, in agreement with the BET surface area and XRD patterns (Figure 2). The addition of chitosan appears to have provided a surface coating and condensed network with the adsorbent particles, thereby enhancing the mechanochemical properties of the organic−inorganic composites. In previous studies,[67,68] the incorporation of the biopolymer was found to accelerate the sol−gel process and influence the microstructure of the final composite material. Through the sol−gel process, chitosan was reported to form cross-linked networks that enhance the structural and surface properties of alkali-activated materials.[58] The effects of the

https://doi.org/10.1021/acs.langmuir.1c01829
Langmuir 2022, 38, 903−913

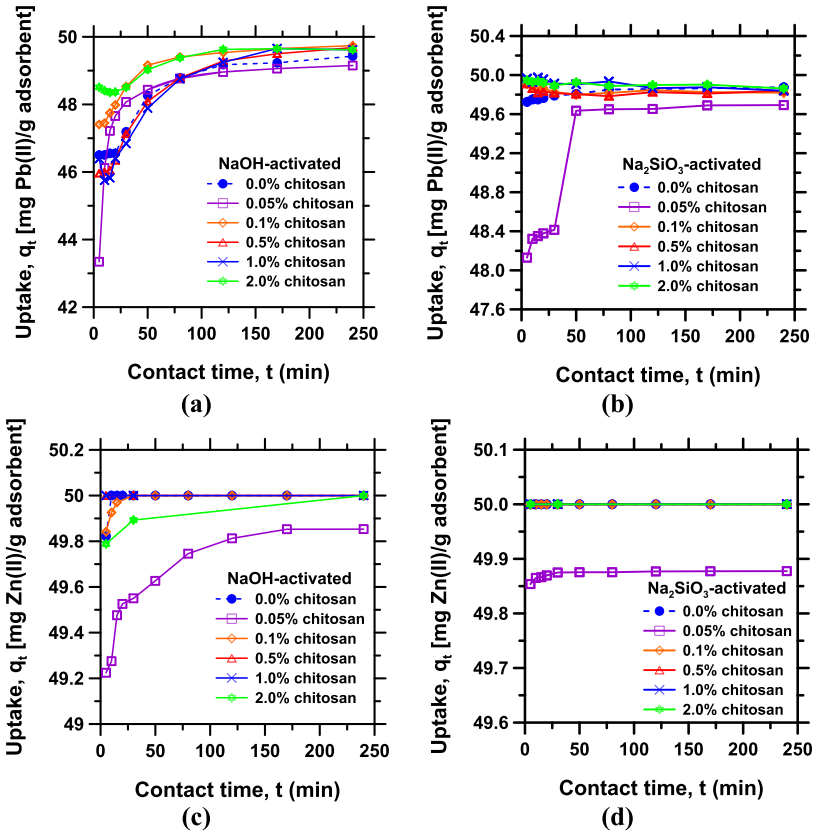

Figure 5. Time-dependent Pb(II) and Zn(II) uptake with the prepared adsorbents: (a and b) Pb(II) and (c and d) Zn(II). The highest possible uptake limit for 100 ppm with 2 g of adsorbent/L is 50 mg/g.

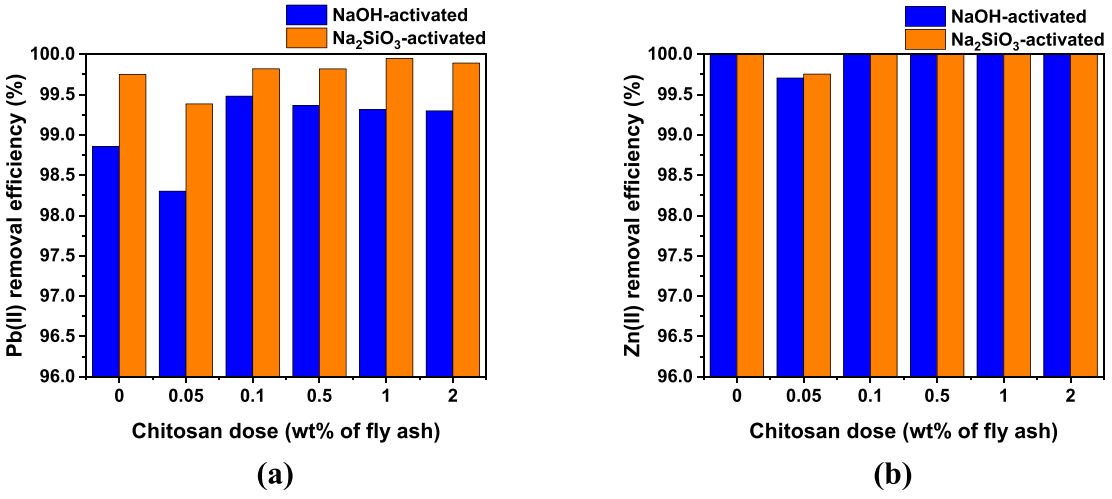

Figure 6. Effect of chitosan dosage on the metal ion removal efficiency of the adsorbents: (a) Pb(II) and (b) Zn(II).

microstructural and surface differences of the two sets of prepared adsorbents are observed on the Pb(II) and Zn(II) sorption performances discussed in Sorption Performance and Effect of Chitosan.

Figure 4 shows the FTIR spectra of chitosan, fly ash, and the prepared hybrid adsorbents before and after metal ion sorption. The chitosan infrared absorption spectra show the characteristic functional groups. The peak at 426 cm^{-1} is assigned to the amide group. The peaks at 1020 and 1050 cm^{-1} are due to the skeletal vibration, including C−O stretching. The peak at 1150 cm^{-1} is designated for antisymmetric stretching of the C−O−C bridge. The absorption bands at 1380, 1430, 1590, and 1670 cm^{-1} are associated with the presence of the C−H bending, OH bending, and bending vibrations of the N−H (N-acetylated residues, amide II band) and C═O stretching of the amide I band, respectively. The C−H stretching vibrations occur at 2860 cm^{-1}, and the −OH bond of the chitosan was found at 3380 cm^{-1}.[69,70] Also, as shown in Figure 4, the main absorption band of the fly ash precursor or the inorganic adsorbent component centered at 960−1000 cm^{-1} is assigned to Si−O−Si or Al−O−Si asymmetric stretching, respectively, and the band at ∼430 cm^{-1} is assigned to the M−O stretching vibration (where M = Al or Si).[71−74] From fly ash samples to the alkali-activated materials, the absorption bands became sharper and slightly

https://doi.org/10.1021/acs.langmuir.1c01829
Langmuir 2022, 38, 903−913

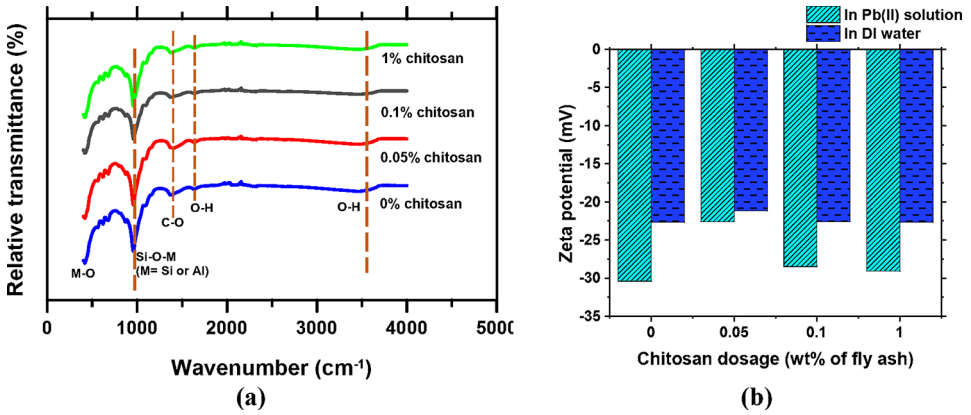

Figure 7. (a) FTIR of chitosan-modified NaOH-activated materials after Pb(II) adsorption. (b) ζ potential of chitosan NaOH-activated materials in deionized water and in a 100 ppm Pb(II) solution.

shifted to lower frequencies. New absorption bands occur in the spectra of the adsorbents at 3400 and 1400 cm^{-1}, assigned to the −OH stretching vibration and O−H bending of structural H_2O and OH of the hydrated adsorbent phases.[75−77] The absorption bands at 1435 cm^{-1} represent C−O stretching of carbonates formed due to atmospheric CO_2 contamination.[76,77] An examination of the FTIR of the adsorbents before and after Pb(II) and Zn(II) sorption shows a slight shift, a reduction, or the disappearance of some functional groups, indicating the sites of chemisorption. For example, we observed in most cases that some of the functional groups (e.g., O−H) seen in the prepared adsorbent disappeared after metal ion adsorption (Figure 4). In the case of Zn(II) adsorption, the absence of O−H and C−O bands implies more adsorption of the metal ions than in the case of Pb(II), as depicted in Figure 4.

Sorption Performance and Effect of Chitosan. The effects of chitosan dosage on the Pb(II) and Zn(II) uptake rate and removal efficiency were studied. Figure 5 shows Pb(II) and Zn(II) uptake as a function of contact time from 5 to 240 min. In this study, the highest possible uptake limit in each of the batch sorption process is 50 $mg_{\text{heavy metal ions [Pb(II) or Zn(II)]}}/g_{\text{adsorbent}}$. As shown in Figure 5, the uptake rate for Pb(II) and Zn(II) was rapid, and in most cases, the sorption had approached equilibrium within the first 5 min. The metal ion uptake of the Na_2SiO_3-activated materials was more rapid than that of the NaOH-activated materials. Also, Zn(II) uptake appears to be faster and higher than Pb(II) uptake, which could be attributable to the small ionic radius and higher change density of Zn(II). The 0.05% chitosan-modified materials generally show poorer performance than the rest of the adsorbents in each set. To understand the effect of chitosan dosage in the two sets of materials, the efficiency of metal ion sorption at a 240 min equilibration time was determined for all of the adsorbents, according to eq 1 and as presented in Figure 6. As shown in Figure 6a, the Pb(II) sorption efficiency of the materials is mostly >98%, and the addition of chitosan at a ≥0.1% dose imparted a slight improvement on the Pb(II) sorption efficiency compared to that with the adsorbent containing 0% chitosan. However, a depression is observed at 0.05%$_{\text{mass}}$ chitosan. The data acquired with the ICP-OES instrument were mostly self-consistent, with relative standard deviation values in the range of ±5%. In comparison, the standard deviations of the measured Zn(II) concentrations were slightly better (lower) than that of the Pb(II) concentrations.

In general, the Na_2SiO_3-activated materials performed better than the NaOH-activated materials. The trend in the sorption performance, as shown in Figure 6, is in agreement with the microstructural properties of the adsorbent discussed in Characterization of Prepared Adsorbents, suggesting that the large surface area and the high amorphous geopolymer-like phase composition of the Na_2SiO_3-activated system may have contributed to its better performance. All of the materials displayed ∼100% Zn(II) removal efficiency at 240 min, except the adsorbent containing 0.05%$_{\text{mass}}$ chitosan, which similarly shows decrease in performance (Figure 6b). It was not clear why there was a decrease at 0.05%$_{\text{mass}}$ chitosan for the NaOH- and Na_2SiO_3-activated systems. A cursory examination of the FTIR of the adsorbents after metal ion adsorption (Figure 7a) shows no difference between the 0.05% and the other chitosan dose rates. However, the literature suggests that the charge density of a biopolymer (e.g., chitosan) can induce quick destabilization and restabilization of the colloidal system through electrostatic interactions.[78,79] The ζ potential of the adsorbents was therefore examined in deionized water and in a metal salt solution, and as shown in Figure 7b, the adsorbent containing 0.05% chitosan has the lowest ζ potential, indicating a lower dispersion stability. Expectedly, the metal ion adsorption decreases with the decreasing negative ζ potential[80] as a result of the decrease in buoyancy and electrostatic interaction of the negatively charged adsorbent surface with the positively charged aqueous metal ions, hence the observed dip at 0.05% chitosan.[80−84]

As shown in Figure 6, the adsorbents prepared in this study displayed high removal efficiencies of 98−100%, corresponding to metal ion uptakes of 49−50 mg/g, under the conditions used in this study. Note that the absolute monolayer maximum adsorption capacity, q_m, was not determined in this study because the scope of this work was to investigate the presence of absence of potential synergy between the geopolymers and various dosages of chitosan biopolymer. Hence, the concentration and other conditions were kept constant while the compositional parameters of the adsorbent materials were varied. To the best of our knowledge, this is the first study of chitosan-modified alkali-activated materials for Pb(II) or Zn(II) ion sorption. Thus, there are limited literature data for appropriate specific comparison with this study. However, the removal efficiency and metal ion uptake found in this study can be compared with the results available in the literature for other geopolymer or alkali-activated materials containing no chitosan, although the chemistry of the adsorbents may differ slightly. For

https://doi.org/10.1021/acs.langmuir.1c01829
Langmuir 2022, 38, 903−913

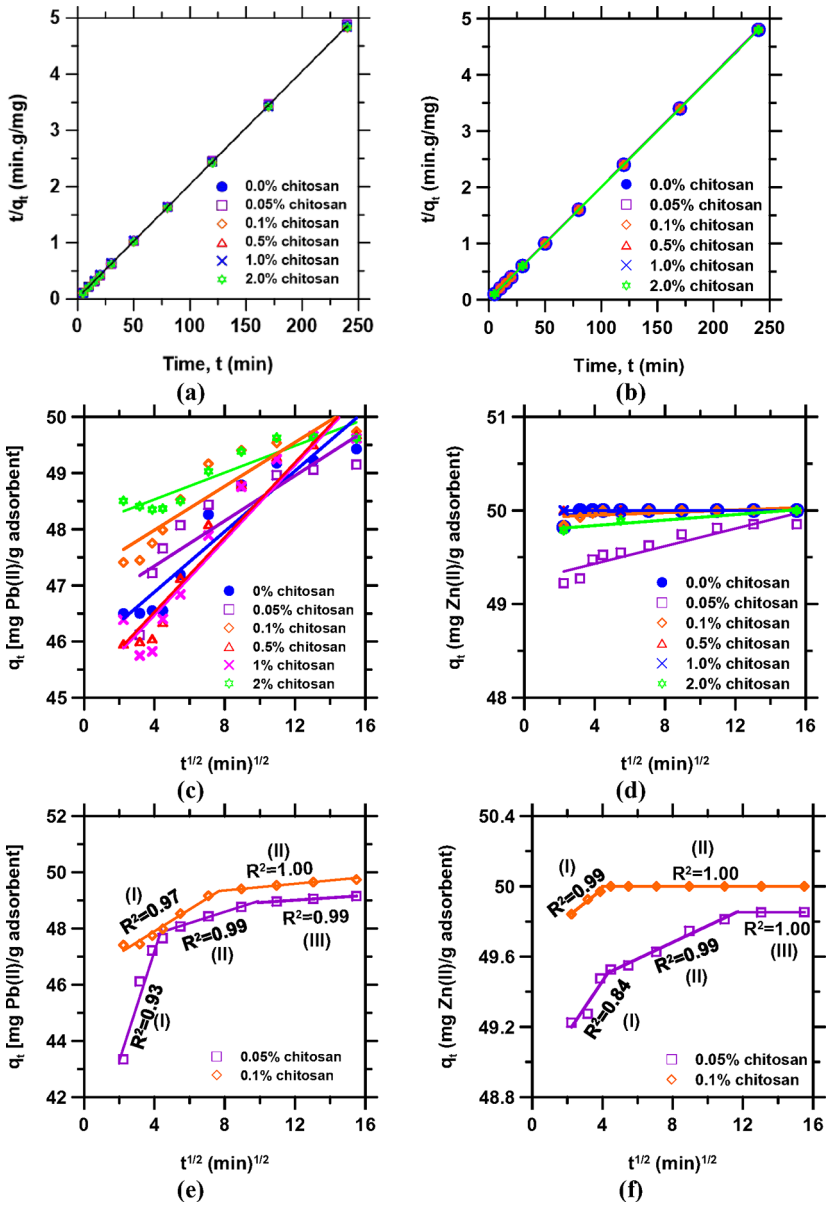

Figure 8. (a and b) Pseudo-second-order kinetic model fitting, (c and d) intraparticle diffusion (IPD) model fitting with a single straight line, and (e and f) intraparticle diffusion (IPD) model fitting with multiple straight lines for Pb(II) and Zn(II) sorption on the NaOH-activated materials, respectively.

example, a 90.66% maximum experimental Pb(II) removal efficiency and a theoretically calculated sorption capacity of ≤182 mg/g were obtained by Al-Zboon et al.[62] using a geopolymer material prepared with a class F fly ash precursor (a low-Ca fly ash containing 15 times less CaO than the fly ash precursor used in this study), and they employed a 14 M NaOH activating solution that is comparable to the activation used for the C1 adsorbent group in this study. Other researchers[85] also prepared adsorbents with class F fly ash, using a mixture of NaOH and a sodium silicate activator (which is similar but a more aggressive activation than the mild activation used for the group C2 adsorbent in this work), and obtained a maximum Pb(II) removal efficiency of 98.4% and a sorption capacity of 24.6 mg/g, using an initial Pb(II) concentration of 100 ppm and a geopolymer dosage of 0.1 g/25 mL. Similarly, a Zn(II) sorption efficiency of 97.7% was reported[86] for alkali-activated material prepared with volcanic tuff and 14 M NaOH, wherein the authors employed an initial Zn(II) ion concentration of 100 ppm and an adsorbent dosage of 0.4 g. They showed that the efficiency drastically decreased with an increase in dosage. A similar initial Zn(II) concentration and a higher adsorbent dosage of 2 g were used in this study, which produced a performance slightly better than those reported by the researchers for the volcanic tuff-based alkali-activated material. A more extensive review of the metal sorption performance of geopolymers prepared with different precursors and various formulation protocols can be found elsewhere.[25,26]

Sorption Mechanism. Due to the presence of amine ($-NH_2$), hydroxyl ($-OH$), and carboxylate ($RCOO^-$) groups in the chitosan, the molecule can interact with the hydration products of alkali-activated materials through chemical association and electrostatic attraction. The FTIR data presented in the preceding sections (Figure 4) show that the adsorbed metal ions interacted with functional groups (e.g., $-OH$) in the hybrid

https://doi.org/10.1021/acs.langmuir.1c01829
Langmuir 2022, 38, 903−913

adsorbents, suggesting a chemisorption phenomenon. On the contrary, the physical surface properties of the adsorbent also may have influenced the sorption process as it was seen that the Na_2SiO_3-activated materials with a larger surface area and a finer pore diameter performed better than the corresponding NaOH-activated materials. To inspect the mechanism of the Pb(II) and Zn(II) sorption process, the data were tested with Lagergren's pseudo-first-order and pseudo-second-order kinetic models expressed in eqs 3 and 4, respectively:[87]

$$\text{first order: } \ln(q_e - q_t) = \ln q_e - k_1 t \tag{3}$$

$$\text{second order: } \frac{t}{q_t} = \frac{1}{k_2 q_e^{\,2}} + \frac{1}{q_e} t \tag{4}$$

where q_e is the uptake at equilibrium, k_1 and k_2 are kinetic constants, and q_t is the uptake at time t. We found that the sorption data fit poorly with the pseudo-first-order model but showed strong fitting to the pseudo-second-order model (Figure 8a,b), suggesting a chemisorption-controlled sorption process.[63,88,89] The results of the kinetic model fittings for the NaOH-activated adsorbents featured a high correlation coefficient ($R^2 \approx 0.999-1.00$) for the pseudo-second-order model fittings.

From the transport perspective, metal ion sorption can be controlled by bulk solution transport, film diffusion, pore diffusion, or a combination of all three.[90−93] Hence, the sorption data were further tested with the intraparticle diffusion (IPD) model shown in eq 5.[94,95]

$$\text{intraparticle diffusion (IPD): } q_t = k_{id} t^{1/2} + \theta \tag{5}$$

where k_{id} is the intraparticle diffusion rate constant (milligrams per gram per half-minute) and θ (milligrams per gram) is a constant related to the boundary layer thickness.[96,97] The sorption is intraparticle diffusion-controlled if the graph of q_t versus $t^{1/2}$ is linear and passes through the origin, indicating a sorption rate that is dependent on the rate at which the metal ions and the adsorbent particles diffuse toward each other.[96,97] However, if the IPD straight line fitting deviates from the graph's origin, it indicates a contribution from a film diffusion process.[92] As shown in panels c and d of Figure 8, the sorption data fit poorly to the single straight line IPD model with R^2 in the wide range of 0.20−1.00. The IPD model fittings do not pass through the origin, which suggests that intraparticle diffusion is not the rate-limiting step, and film diffusion also plays an important role in the process. As exemplified in panels e and f of Figure 8, the IPD model fitting mostly exhibits multilinear features indicating that the sorption is rather influenced by multiple processes[96] and that the process occurs in multiple stages with varying degrees of contributions from intraparticle diffusion and film diffusion.[90−92] As shown in the multilinear fitting of panels e and f of Figure 8, as the deviation of each straight line from the origin increases, the R^2 value increases approaching 1.00, suggesting the growing influence of film diffusion on the kinetic process from stage I to stage III. Thus, in agreement with previous studies,[27,59] the examination presented above suggests the sorption process is controlled mostly by chemisorption, wherein the physicochemical interaction appears to involve concurrent processes, including surface adsorption, precipitation, ion exchange, chemisorption, and concurrent film and intraparticle diffusion.

Although regenerability has not been covered in this study, a few previous studies have shown that a geopolymer-based adsorbent can be made regenerable with appropriate design and fabrication.[98−101]

CONCLUSIONS

Sustainable alkali-activated inorganic−organic composite materials were synthesized utilizing class C fly ash with different chitosan dosages ($0-2\%_{mass}$), and the materials' performance in removing aqueous Pb(II) and Zn(II) was studied. The results show that the addition of chitosan, at a dosage of $\geq 0.1\%_{mass}$, produced a very small improvement in the Pb(II) sorption performance; a 0.05% chitosan dosage led to a general decrease in the sorption performance, but the unmodified alkali-activated material showed removal efficiencies upward of 98% for both Pb(II) and Zn(II). In general, the sodium silicate-activated materials performed better than the sodium hydroxide-activated materials, and all of the materials displayed higher sorption for Zn(II) than for Pb(II). In summary, the chitosan addition may be beneficial, but under the conditions of this study, the improvements in the performance of the alkali-activated materials for aqueous Pb(II) and Zn(II) removal were not significant. However, further studies are needed to fully investigate the performance of these hybrid adsorbents. Recommended areas of further studies include investigation of the effects of varying heavy metal concentrations, temperature and pH, ion selectivity in multi-ion systems, a continuous adsorption process, and regenerability of the chitosan-modified alkali-activated materials compared to the unmodified.

AUTHOR INFORMATION

Corresponding Author

Monday U. Okoronkwo − *Sustainable Materials Laboratory (SusMatLab), Missouri University of Science and Technology, Rolla, Missouri 65409, United States; Department of Chemical and Biochemical Engineering, Missouri University of Science and Technology, Rolla, Missouri 65409, United States;* orcid.org/0000-0001-5033-9860; Phone: 573-341-4349; Email: okoronkwom@mst.edu

Authors

Sukanta K. Mondal − *Sustainable Materials Laboratory (SusMatLab), Missouri University of Science and Technology, Rolla, Missouri 65409, United States; Department of Chemical and Biochemical Engineering, Missouri University of Science and Technology, Rolla, Missouri 65409, United States;* orcid.org/0000-0002-1880-1127

Chenglin Wu − *Department of Civil, Architectural & Environmental Engineering, Missouri University of Science and Technology, Rolla, Missouri 65409, United States;* orcid.org/0000-0001-7733-1084

Felix C. Nwadire − *Department of Chemistry, Michael Okpara University of Agriculture, P.M.B. 7267 Umuahia, Abia, Nigeria*

Ali Rownaghi − *Department of Chemical and Biochemical Engineering, Missouri University of Science and Technology, Rolla, Missouri 65409, United States*

Aditya Kumar − *Department of Materials Science and Engineering, Missouri University of Science and Technology, Rolla, Missouri 65409, United States;* orcid.org/0000-0001-7550-8034

Yusuf Adewuyi − *Department of Chemical, Biological and Bioengineering, North Carolina Agricultural and Technical State University, Greensboro, North Carolina 27411, United States;* orcid.org/0000-0002-2511-4923

https://doi.org/10.1021/acs.langmuir.1c01829
Langmuir 2022, 38, 903−913

Complete contact information is available at:
https://pubs.acs.org/10.1021/acs.langmuir.1c01829

Notes

The authors declare no competing financial interest.

■ ACKNOWLEDGMENTS

Support from the National Science Foundation (CMMI: 1932690) is acknowledged. The experiments were conducted at the Sustainable Materials Laboratory (SusMatLab), Materials Research Center (MRC), and the Center for Research in Energy and Environment (CREE), all at the Missouri University of Science and Technology. The authors thank LafargeHolcim for the supply of fly ash samples.

■ REFERENCES

(1) Sikder, A.; Pearce, A. K.; Parkinson, S. J.; Napier, R.; O'Reilly, R. K. Recent Trends in Advanced Polymer Materials in Agriculture Related Applications. *ACS Appl. Polym. Mater.* **2021**, *3* (3), 1203−1217.
(2) Klein, M.; Poverenov, E. Natural Biopolymer-Based Hydrogels for Use in Food and Agriculture. *J. Sci. Food Agric.* **2020**, *100* (6), 2337−2347.
(3) Udayakumar, G. P.; Muthusamy, S.; Selvaganesh, B.; Sivarajasekar, N.; Rambabu, K.; Banat, F.; Sivamani, S.; Sivakumar, N.; Hosseini-Bandegharaei, A.; Show, P. L. Biopolymers and Composites: Properties, Characterization and Their Applications in Food, Medical and Pharmaceutical Industries. *J. Environ. Chem. Eng.* **2021**, *9* (4), 105322.
(4) Mitura, S.; Sionkowska, A.; Jaiswal, A. Biopolymers for Hydrogels in Cosmetics: Review. *J. Mater. Sci. Mater. Med.* **2020**, *31* (6), 50.
(5) Rehm, B.; Moradali, F. M. *Biopolymers for Biomedical and Biotechnological Applications*; John Wiley & Sons, Ltd.: Weinheim, Germany, 2021; pp 1−376.
(6) Jummaat, F.; Yahya, E. B.; Khalil H. P. S, A.; Adnan, A. S.; Alqadhi, A. M.; Abdullah, C. K.; A. K, A. S.; Olaiya, N. G.; Abdat, M. The Role of Biopolymer-Based Materials in Obstetrics and Gynecology Applications: A Review. *Polymers* **2021**, *13* (4), 633.
(7) Niaounakis, M. *Biopolymers: Applications and Trends*; William Andrew Publishing: Oxford, U.K., 2015; pp 233−255.
(8) Plank, J. Applications of Biopolymers and Other Biotechnological Products in Building Materials. *Appl. Microbiol. Biotechnol.* **2004**, *66* (1), 1−9.
(9) Pacheco-Torgal, F.; Ivanov, V.; Karak, N.; Jonkers, H. *Biopolymers and Biotech Admixtures for Eco-Efficient Construction Materials*; Elsevier: Duxford, U.K., 2016; pp 1−271.
(10) Zia, Z.; Hartland, A.; Mucalo, M. R. Use of Low-Cost Biopolymers and Biopolymeric Composite Systems for Heavy Metal Removal from Water. *Int. J. Environ. Sci. Technol.* **2020**, *17* (10), 4389−4406.
(11) Galiano, F.; Briceño, K.; Marino, T.; Molino, A.; Christensen, K. V.; Figoli, A. Advances in Biopolymer-Based Membrane Preparation and Applications. *J. Membr. Sci.* **2018**, *564*, 562−586.
(12) Jaiswal, A.; Ghsoh, S. S.; Chattopadhyay, A. Quantum Dot Impregnated-Chitosan Film for Heavy Metal Ion Sensing and Removal. *Langmuir* **2012**, *28* (44), 15687−15696.
(13) Ahmad, M.; Ahmed, S.; Swami, B. L.; Ikram, S. Adsorption of Heavy Metal Ions: Role of Chitosan and Cellulose for Water Treatment. *IJP* **2015**, *6* (2), 280−289.
(14) Kurita, K. Chitin and Chitosan: Functional Biopolymers from Marine Crustaceans. *Mar. Biotechnol.* **2006**, *8* (3), 203.
(15) Younes, I.; Rinaudo, M. Chitin and Chitosan Preparation from Marine Sources. Structure, Properties and Applications. *Mar. Drugs* **2015**, *13* (3), 1133−1174.
(16) Sarode, S.; Upadhyay, P.; Khosa, M. A.; Mak, T.; Shakir, A.; Song, S.; Ullah, A. Overview of Wastewater Treatment Methods with Special Focus on Biopolymer Chitin-Chitosan. *Int. J. Biol. Macromol.* **2019**, *121*, 1086−1100.
(17) Zhang, L.; Zeng, Y.; Cheng, Z. Removal of Heavy Metal Ions Using Chitosan and Modified Chitosan: A Review. *J. Mol. Liq.* **2016**, *214*, 175−191.
(18) Li, N.; Bai, R.; Liu, C. Enhanced and Selective Adsorption of Mercury Ions on Chitosan Beads Grafted with Polyacrylamide via Surface-Initiated Atom Transfer Radical Polymerization. *Langmuir* **2005**, *21* (25), 11780−11787.
(19) Yang, H.; Sheikhi, A.; Van De Ven, T. G. Reusable Green Aerogels from Cross-Linked Hairy Nanocrystalline Cellulose and Modified Chitosan for Dye Removal. *Langmuir* **2016**, *32* (45), 11771−11779.
(20) Kuang, S.-P.; Wang, Z.-Z.; Liu, J.; Wu, Z.-C. Preparation of Triethylene-Tetramine Grafted Magnetic Chitosan for Adsorption of Pb(II) Ion from Aqueous Solutions. *J. Hazard. Mater.* **2013**, *260*, 210−219.
(21) Liu, X.; Hu, Q.; Fang, Z.; Zhang, X.; Zhang, B. Magnetic Chitosan Nanocomposites: A Useful Recyclable Tool for Heavy Metal Ion Removal. *Langmuir* **2009**, *25* (1), 3−8.
(22) Pontoni, L.; Fabbricino, M. Use of Chitosan and Chitosan-Derivatives to Remove Arsenic from Aqueous Solutions—a Mini Review. *Carbohydr. Res.* **2012**, *356*, 86−92.
(23) Vakili, M.; Rafatullah, M.; Salamatinia, B.; Abdullah, A. Z.; Ibrahim, M. H.; Tan, K. B.; Gholami, Z.; Amouzgar, P. Application of Chitosan and Its Derivatives as Adsorbents for Dye Removal from Water and Wastewater: A Review. *Carbohydr. Polym.* **2014**, *113*, 115−130.
(24) Biswas, S.; Fatema, J.; Debnath, T.; Rashid, T. U. Chitosan−Clay Composites for Wastewater Treatment: A State-of-the-Art Review. *ACS EST Water* **2021**, *1* (5), 1055−1085.
(25) Siyal, A. A.; Shamsuddin, M. R.; Khan, M. I.; Rabat, N. E.; Zulfiqar, M.; Man, Z.; Siame, J.; Azizli, K. A. A Review on Geopolymers as Emerging Materials for the Adsorption of Heavy Metals and Dyes. *J. Environ. Manage.* **2018**, *224*, 327−339.
(26) Tan, T. H.; Mo, K. H.; Ling, T.-C.; Lai, S. H. Current Development of Geopolymer as Alternative Adsorbent for Heavy Metal Removal. *Environ. Technol. Innov.* **2020**, *18*, 100684.
(27) Mondal, S. K.; Welz, A.; Rezaei, F.; Kumar, A.; Okoronkwo, M. U. Structure−Property Relationship of Geopolymers for Aqueous Pb Removal. *ACS Omega* **2020**, *5* (34), 21689−21699.
(28) Adewuyi, Y. G. Recent Advances in Fly-Ash-Based Geopolymers: Potential on the Utilization for Sustainable Environmental Remediation. *ACS Omega* **2021**, *6* (24), 15532−15542.
(29) Davidovits, J. Geopolymers: Inorganic Polymeric New Materials. *J. Therm. Anal.* **1991**, *37* (8), 1633−1656.
(30) Provis, J. L.; Van Deventer, J. S. J. *Geopolymers: Structures, Processing, Properties and Industrial Applications*; Woodhead Publishing: Oxford, U.K., 2009; pp 15−136.
(31) Provis, J. L.; Rose, V.; Bernal, S. A.; van Deventer, J. S. J. High-Resolution Nanoprobe X-Ray Fluorescence Characterization of Heterogeneous Calcium and Heavy Metal Distributions in Alkali-Activated Fly Ash. *Langmuir* **2009**, *25* (19), 11897−11904.
(32) Steins, P.; Poulesquen, A.; Diat, O.; Frizon, F. Structural Evolution during Geopolymerization from an Early Age to Consolidated Material. *Langmuir* **2012**, *28* (22), 8502−8510.
(33) The American Coal Ash Association. About Coal Ash. https://acaa-usa.org/about-coal-ash/faqs/ (accessed 2021-06-24).
(34) Alibaba.com. Chitosan Manufacturers. Suppliers and Exporters on Alibaba.com. https://www.alibaba.com/trade/ (accessed 2021-06-11).
(35) Zuorro, A.; Moreno-Sader, K. A.; González-Delgado, Á. D. Economic Evaluation and Techno-Economic Sensitivity Analysis of a Mass Integrated Shrimp Biorefinery in North Colombia. *Polymers* **2020**, *12* (10), 2397.
(36) Ensymm. Chitosan Product Line Offer. 2010. https://www.sumanfoodconsultants.com (accessed 2021-06-24).
(37) Meramo-Hurtado, S. I.; González-Delgado, Á. D. Application of Techno-Economic and Sensitivity Analyses as Decision-Making Tools for Assessing Emerging Large-Scale Technologies for Production of Chitosan-Based Adsorbents. *ACS Omega* **2020**, *5* (28), 17601−17610.

(38) Ahmaruzzaman, M. A Review on the Utilization of Fly Ash. *Prog. Energy Combust. Sci.* **2010**, *36* (3), 327−363.
(39) Scheetz, B. E.; Earle, R. Utilization of Fly Ash. *Curr. Opin. Solid State Mater. Sci.* **1998**, *3* (5), 510−520.
(40) Huang, T. Y.; Chiueh, P. T.; Lo, S. L. Life-Cycle Environmental and Cost Impacts of Reusing Fly Ash. *Resour. Conserv. Recycl.* **2017**, *123*, 255−260.
(41) Qiu, B.; Peng, L.; Xu, X.; Lin, X.; Hong, J.; Huo, X. Medical Investigation of E-Waste Demanufacturing Industry in Guiyu Town. Greenpeace and Chinese Society for Environmental Sciences: Beijing, 2004; pp 79−83.
(42) Hall, S. Lead Pollution and Poisoning. *Environ. Sci. Technol.* **1972**, *6* (1), 30−35.
(43) Roy, N. K.; Rossman, T. G. Mutagenesis and Comutagenesis by Lead Compounds. *Mutat. Res. Toxicol.* **1992**, *298* (2), 97−103.
(44) *Guidelines for Drinking-Water Quality*; World Health Organization, 1993.
(45) Lanphear, B. P.; Hornung, R.; Khoury, J.; Yolton, K.; Baghurst, P.; Bellinger, D. C.; Canfield, R. L.; Dietrich, K. N.; Bornschein, R.; Greene, T.; Rothenberg, S. J.; Needleman, H. L.; Schnaas, L.; Wasserman, G.; Graziano, J.; Roberts, R. Low-Level Environmental Lead Exposure and Children's Intellectual Function: An International Pooled Analysis. *Environ. Health Perspect.* **2005**, *113* (7), 894−899.
(46) Flora, G.; Gupta, D.; Tiwari, A. Toxicity of Lead: A Review with Recent Updates. *Interdiscip. Toxicol.* **2012**, *5* (2), 47−58.
(47) Fu, F.; Wang, Q. Removal of Heavy Metal Ions from Wastewaters: A Review. *J. Environ. Manage.* **2011**, *92* (3), 407−418.
(48) Hojati, S.; Landi, A. Kinetics and Thermodynamics of Zinc Removal from a Metal-Plating Wastewater by Adsorption onto an Iranian Sepiolite. *Int. J. Environ. Sci. Technol.* **2015**, *12* (1), 203−210.
(49) Doncheva, S.; Stoynova, Z.; Velikova, V. Influence of Succinate on Zinc Toxicity of Pea Plants. *J. Plant Nutr.* **2001**, *24* (6), 789−804.
(50) Bonnet, M.; Camares, O.; Veisseire, P. Effects of Zinc and Influence of Acremonium Lolii on Growth Parameters, Chlorophyll a Fluorescence and Antioxidant Enzyme Activities of Ryegrass (Lolium Perenne L. Cv Apollo). *J. Exp. Bot.* **2000**, *51* (346), 945−953.
(51) Hart, B. T. *A Compilation of Australian Water Quality Criteria*; 1974.
(52) Plum, L. M.; Rink, L.; Haase, H. The Essential Toxin: Impact of Zinc on Human Health. *Int. J. Environ. Res. Public. Health* **2010**, *7* (4), 1342−1365.
(53) Igic, P. G.; Lee, E.; Harper, W.; Roach, K. W. *Toxic Effects Associated with Consumption of Zinc*; Elsevier, 2002; Vol. *77*, pp 713−716.
(54) Guibal, E. Interactions of Metal Ions with Chitosan-Based Sorbents: A Review. *Sep. Purif. Technol.* **2004**, *38* (1), 43−74.
(55) Okoronkwo, M. U.; Balonis, M.; Katz, L.; Juenger, M.; Sant, G. A Thermodynamics-Based Approach for Examining the Suitability of Cementitious Formulations for Solidifying and Stabilizing Coal-Combustion Wastes. *J. Environ. Manage.* **2018**, *217*, 278−287.
(56) Skorina, T. Ion Exchange in Amorphous Alkali-Activated Aluminosilicates: Potassium Based Geopolymers. *Appl. Clay Sci.* **2014**, *87*, 205−211.
(57) Chen, X.; Niu, Z.; Zhang, H.; Lu, M.; Lu, Y.; Zhou, M.; Li, B. Design of a Chitosan Modifying Alkali-Activated Slag Pervious Concrete with the Function of Water Purification. *Constr. Build. Mater.* **2020**, *251*, 118979.
(58) Li, Z.; Chen, R.; Zhang, L. Utilization of Chitosan Biopolymer to Enhance Fly Ash-Based Geopolymer. *J. Mater. Sci.* **2013**, *48* (22), 7986−7993.
(59) Mondal, S. K.; Welz, A.; Rownaghi, A.; Wang, B.; Ma, H.; Rezaei, F.; Kumar, A.; Okoronkwo, M. U. Investigating the Microstructure of High-Calcium Fly Ash-Based Alkali-Activated Material for Aqueous Zn Sorption. *Environ. Res.* **2021**, *198*, 110484.
(60) Al-Harahsheh, M. S.; Al Zboon, K.; Al-Makhadmeh, L.; Hararah, M.; Mahasneh, M. Fly Ash Based Geopolymer for Heavy Metal Removal: A Case Study on Copper Removal. *J. Environ. Chem. Eng.* **2015**, *3* (3), 1669−1677.
(61) Kara, I.; Yilmazer, D.; Akar, S. T. Metakaolin Based Geopolymer as an Effective Adsorbent for Adsorption of Zinc (II) and Nickel (II) Ions from Aqueous Solutions. *Appl. Clay Sci.* **2017**, *139*, 54−63.
(62) Al-Zboon, K.; Al-Harahsheh, M. S.; Hani, F. B. Fly Ash-Based Geopolymer for Pb Removal from Aqueous Solution. *J. Hazard. Mater.* **2011**, *188* (1−3), 414−421.
(63) Ho, Y.-S. Review of Second-Order Models for Adsorption Systems. *J. Hazard. Mater.* **2006**, *136* (3), 681−689.
(64) Thommes, M.; Kaneko, K.; Neimark, A. V.; Olivier, J. P.; Rodriguez-Reinoso, F.; Rouquerol, J.; Sing, K. S. W. Physisorption of Gases, with Special Reference to the Evaluation of Surface Area and Pore Size Distribution (IUPAC Technical Report). *Pure Appl. Chem.* **2015**, *87* (9−10), 1051−1069.
(65) Duxson, P.; Fernández-Jiménez, A.; Provis, J. L.; Lukey, G. C.; Palomo, A.; van Deventer, J. S. J. Geopolymer Technology: The Current State of the Art. *J. Mater. Sci.* **2007**, *42* (9), 2917−2933.
(66) Bernal, S. A.; Provis, J. L.; Fernández-Jiménez, A.; Krivenko, P. V.; Kavalerova, E.; Palacios, M.; Shi, C. Binder Chemistry − High-Calcium Alkali-Activated Materials. In *Alkali Activated Materials: State-of-the-Art Report, RILEM TC 224-AAM*; Provis, J. L., van Deventer, J. S. J., Eds.; RILEM State-of-the-Art Reports; Springer: Dordrecht, The Netherlands, 2014; pp 59−91. DOI: 10.1007/978-94-007-7672-2_3
(67) Shchipunov, Y. A. Sol−Gel-Derived Biomaterials of Silica and Carrageenans. *J. Colloid Interface Sci.* **2003**, *268* (1), 68−76.
(68) Shchipunov, Y. A.; Karpenko, T. Y. Hybrid Polysaccharide- Silica Nanocomposites Prepared by the Sol- Gel Technique. *Langmuir* **2004**, *20* (10), 3882−3887.
(69) Yasmeen, S.; Kabiraz, M. K.; Saha, B.; Qadir, M. R.; Gafur, M. A.; Masum, S. M. Chromium (VI) Ions Removal from Tannery Effluent Using Chitosan-Microcrystalline Cellulose Composite as Adsorbent. *Int. Res. J. Pure Appl. Chem.* **2016**, *10*, 1−14.
(70) AbdElhady, M. Preparation and Characterization of Chitosan/Zinc Oxide Nanoparticles for Imparting Antimicrobial and UV Protection to Cotton Fabric. *Int. J. Carbohydr. Chem.* **2012**, *2012*, 1−6.
(71) Lee, W. K. W.; van Deventer, J. S. J. Use of Infrared Spectroscopy to Study Geopolymerization of Heterogeneous Amorphous Aluminosilicates. *Langmuir* **2003**, *19* (21), 8726−8734.
(72) Álvarez-Ayuso, E.; Querol, X.; Plana, F.; Alastuey, A.; Moreno, N.; Izquierdo, M.; Font, O.; Moreno, T.; Diez, S.; Vázquez, E.; Barra, M. Environmental, Physical and Structural Characterisation of Geopolymer Matrixes Synthesised from Coal (Co-) Combustion Fly Ashes. *J. Hazard. Mater.* **2008**, *154* (1−3), 175−183.
(73) He, K.; Chen, Y.; Tang, Z.; Hu, Y. Removal of Heavy Metal Ions from Aqueous Solution by Zeolite Synthesized from Fly Ash. *Env. Sci. Pollut Res. Int.* **2016**, *23* (3), 2778−2788.
(74) Mužek, M. N.; Svilović, S.; Ugrina, M.; Zelić, J. Removal of Copper and Cobalt Ions by Fly Ash-Based Geopolymer from Solutions-Equilibrium Study. *Desalination Water Treat.* **2016**, *57* (23), 10689−10699.
(75) Rees, C. A.; Provis, J. L.; Lukey, G. C.; van Deventer, J. S. J. In Situ ATR-FTIR Study of the Early Stages of Fly Ash Geopolymer Gel Formation. *Langmuir* **2007**, *23* (17), 9076−9082.
(76) Álvarez-Ayuso, E.; Querol, X.; Plana, F.; Alastuey, A.; Moreno, N.; Izquierdo, M.; Font, O.; Moreno, T.; Diez, S.; Vázquez, E.; Barra, M. Environmental, Physical and Structural Characterisation of Geopolymer Matrixes Synthesised from Coal (Co-)Combustion Fly Ashes. *J. Hazard. Mater.* **2008**, *154* (1), 175−183.
(77) García-Lodeiro, I.; Fernández-Jiménez, A.; Blanco, M. T.; Palomo, A. FTIR Study of the Sol−Gel Synthesis of Cementitious Gels: C−S−H and N−A−S−H. *J. Sol-Gel Sci. Technol.* **2008**, *45* (1), 63−72.
(78) Ashraf, M.; Batool, S.; Ahmad, M.; Sarfraz, M.; Noor, W. S. A. W. M. Biopolymers as Biofilters and Biobarriers. In *Biopolymers and Biotech Admixtures for Eco-Efficient Construction Materials*; Elsevier, 2016; pp 387−420.
(79) Tsai, S.; Lin, C.; Wu, C.; Xin, B. Cell Immobilization Technique for Biotrickle Filtering of Isopropyl Alcohol Waste Vapor Generated by High□technology Industries. *J. Chem. Technol. Biotechnol.* **2013**, *88* (3), 364−371.

https://doi.org/10.1021/acs.langmuir.1c01829
Langmuir 2022, 38, 903−913

(80) He, C.; Xie, F. Adsorption Behavior of Manganese Dioxide towards Heavy Metal Ions: Surface Zeta Potential Effect. *Water, Air, Soil Pollut.* **2018**, *229* (3), 77.
(81) Gunasekara, C.; Law, D. W.; Setunge, S.; Sanjayan, J. G. Zeta Potential, Gel Formation and Compressive Strength of Low Calcium Fly Ash Geopolymers. *Constr. Build. Mater.* **2015**, *95*, 592−599.
(82) Sadowski, Z. Effect of Biosorption of Pb(II), Cu(II) and Cd(II) on the Zeta Potential and Flocculation of Nocardia Sp. *Miner. Eng.* **2001**, *14* (5), 547−552.
(83) Erdemoglu, M.; Sarikaya, M. Effects of Heavy Metals and Oxalate on the Zeta Potential of Magnetite. *J. Colloid Interface Sci.* **2006**, *300* (2), 795−804.
(84) Savaji, K. V.; Niitsoo, O.; Couzis, A. Influence of Particle/Solid Surface Zeta Potential on Particle Adsorption Kinetics. *J. Colloid Interface Sci.* **2014**, *431*, 165−175.
(85) Liu, Y.; Yan, C.; Zhang, Z.; Wang, H.; Zhou, S.; Zhou, W. A Comparative Study on Fly Ash, Geopolymer and Faujasite Block for Pb Removal from Aqueous Solution. *Fuel* **2016**, *185*, 181−189.
(86) Al-Zboon, K. K.; Al-Smadi, B. M.; Al-Khawaldh, S. Natural Volcanic Tuff-Based Geopolymer for Zn Removal: Adsorption Isotherm, Kinetic, and Thermodynamic Study. *Water, Air, Soil Pollut.* **2016**, *227* (7), 248.
(87) Sen Gupta, S.; Bhattacharyya, K. G. Kinetics of Adsorption of Metal Ions on Inorganic Materials: A Review. *Adv. Colloid Interface Sci.* **2011**, *162* (1−2), 39−58.
(88) Ho, Y.-S.; McKay, G. Pseudo-Second Order Model for Sorption Processes. *Process Biochem.* **1999**, *34* (5), 451−465.
(89) Ofomaja, A. E.; Naidoo, E. B.; Modise, S. J. Kinetic and Pseudo-Second-Order Modeling of Lead Biosorption onto Pine Cone Powder. *Ind. Eng. Chem. Res.* **2010**, *49* (6), 2562−2572.
(90) Chaudhry, S. A.; Khan, T. A.; Ali, I. Adsorptive Removal of Pb(II) and Zn(II) from Water onto Manganese Oxide-Coated Sand: Isotherm, Thermodynamic and Kinetic Studies. *Egypt. J. Basic Appl. Sci.* **2016**, *3* (3), 287−300.
(91) Chaudhry, S. A.; Khan, T. A.; Ali, I. Equilibrium, Kinetic and Thermodynamic Studies of Cr(VI) Adsorption from Aqueous Solution onto Manganese Oxide Coated Sand Grain (MOCSG). *J. Mol. Liq.* **2017**, *236*, 320−330.
(92) Khan, T. A.; Chaudhry, S. A.; Ali, I. Equilibrium Uptake, Isotherm and Kinetic Studies of Cd(II) Adsorption onto Iron Oxide Activated Red Mud from Aqueous Solution. *J. Mol. Liq.* **2015**, *202*, 165−175.
(93) Singh, S. K.; Townsend, T. G.; Mazyck, D.; Boyer, T. H. Equilibrium and Intra-Particle Diffusion of Stabilized Landfill Leachate onto Micro- and Meso-Porous Activated Carbon. *Water Res.* **2012**, *46* (2), 491−499.
(94) Simonin, J.-P.; Bouté, J. Intraparticle Diffusion-Adsorption Model to Describe Liquid/Solid Adsorption Kinetics. *Rev. Mex. Ing. Quím.* **2016**, *15* (1), 161−173.
(95) Wu, F.-C.; Tseng, R.-L.; Juang, R.-S. Initial Behavior of Intraparticle Diffusion Model Used in the Description of Adsorption Kinetics. *Chem. Eng. J.* **2009**, *153* (1−3), 1−8.
(96) Fierro, V.; Torné-Fernández, V.; Montané, D.; Celzard, A. Adsorption of Phenol onto Activated Carbons Having Different Textural and Surface Properties. *Microporous Mesoporous Mater.* **2008**, *111* (1−3), 276−284.
(97) Kannan, N.; Sundaram, M. M. Kinetics and Mechanism of Removal of Methylene Blue by Adsorption on Various Carbons—a Comparative Study. *Dyes Pigments* **2001**, *51* (1), 25−40.
(98) Maleki, A.; Hajizadeh, Z.; Sharifi, V.; Emdadi, Z. A Green, Porous and Eco-Friendly Magnetic Geopolymer Adsorbent for Heavy Metals Removal from Aqueous Solutions. *J. Clean. Prod.* **2019**, *215*, 1233−1245.
(99) Kaewmee, P.; Song, M.; Iwanami, M.; Tsutsumi, H.; Takahashi, F. Porous and Reusable Potassium-Activated Geopolymer Adsorbent with High Compressive Strength Fabricated from Coal Fly Ash Wastes. *J. Clean. Prod.* **2020**, *272*, 122617.
(100) Heponiemi, A.; Pesonen, J.; Hu, T.; Lassi, U. Alkali-Activated Materials as Catalysts for Water Purification. *Catalysts* **2021**, *11*, 664.
(101) Sundhararasu, E.; Tuomikoski, S.; Runtti, H.; Hu, T.; Varila, T.; Kangas, T.; Lassi, U. Alkali-Activated Adsorbents from Slags: Column Adsorption and Regeneration Study for Nickel (II) Removal. *ChemEngineering* **2021**, *5* (1), 13.

https://doi.org/10.1021/acs.langmuir.1c01829
Langmuir 2022, 38, 903−913